The official journal of
INTERNATIONAL FEDERATION OF PIGMENT CELL SOCIETIES · SOCIETY FOR MELANOMA RESEARCH

PIGMENT CELL & MELANOMA Research

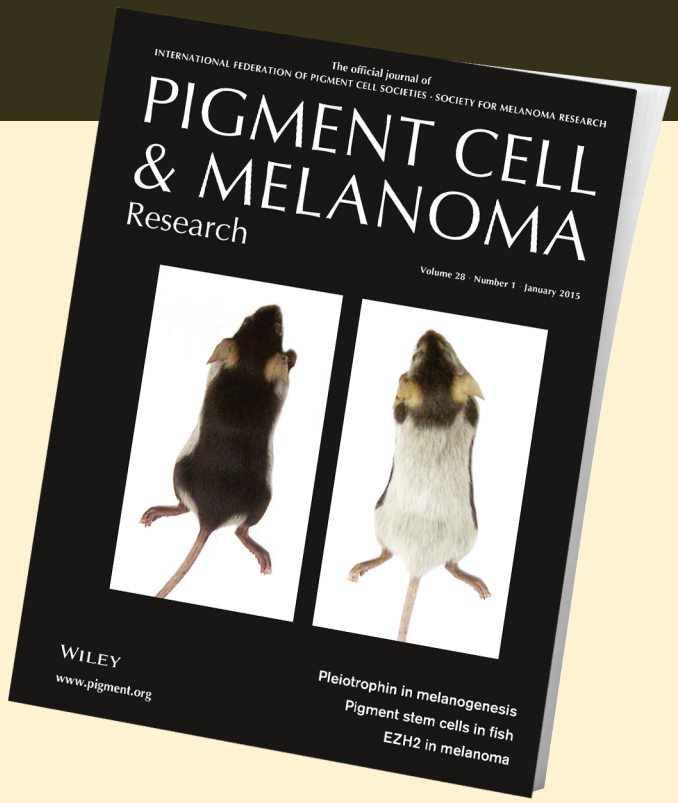

Role of the cystathionine γ lyase/hydrogen sulfide pathway in human melanoma progression

Elisabetta Panza, Paola De Cicco, Chiara Armogida, Giosuè Scognamiglio, Vincenzo Gigantino, Gerardo Botti, Domenico Germano, Maria Napolitano, Andreas Papapetropoulos, Mariarosaria Bucci, Giuseppe Cirino and Angela Ianaro

DOI: 10.1111/pcmr.12312

Volume 28, Issue 1, Pages 61–72

If you wish to order reprints of this article, please see the guidelines **here**

Supporting Information for this article is freely available **here**

EMAIL ALERTS

Receive free email alerts and stay up-to-date on what is published in Pigment Cell & Melanoma Research – **click here**

Submit your next paper to PCMR online at http://mc.manuscriptcentral.com/pcmr

Subscribe to PCMR and stay up-to-date with the only journal committed to publishing basic research in melanoma and pigment cell biology

As a member of the IFPCS or the SMR you automatically get online access to PCMR. Sign up as a member today at **www.ifpcs.org** or at **www.societymelanomaresarch.org**

To take out a personal subscription, please click here

More information about Pigment Cell & Melanoma Research at **www.pigment.org**

Role of the cystathionine γ lyase/hydrogen sulfide pathway in human melanoma progression

Elisabetta Panza[1], Paola De Cicco[1], Chiara Armogida[1], Giosuè Scognamiglio[2], Vincenzo Gigantino[2], Gerardo Botti[2], Domenico Germano[3], Maria Napolitano[4], Andreas Papapetropoulos[5], Mariarosaria Bucci[1], Giuseppe Cirino[1] and Angela Ianaro[1]

1 Department of Pharmacy, University of Naples Federico II, Naples, Italy **2** Unit of Pathology, Istituto Nazionale per lo Studio e la cura dei tumori Fondazione G. Pascale IRCCS, Naples, Italy **3** Oncology Unit, G. Rummo Hospital, Benevento, Italy **4** Department of Oncological Immunology, Istituto Nazionale per lo Studio e la cura dei tumori Fondazione Giovanni Pascale IRCCS, Naples, Italy **5** Faculty of Pharmacy, University of Athens, Athens, Greece

CORRESPONDENCE Giuseppe Cirino, e-mail: cirino@unina.it

KEYWORDS apoptosis/cystathionine γ lyase/hydrogen sulfide/melanoma/nuclear factor-κB

PUBLICATION DATA Received 25 February 2014, revised and accepted for publication 26 August 2014, published online 9 September 2014

doi: 10.1111/pcmr.12312

Summary

In humans, two main metabolic enzymes synthesize hydrogen sulfide (H_2S): cystathionine γ lyase (CSE) and cystathionine β synthase (CBS). A third enzyme, 3-mercaptopyruvate sulfurtransferase (3-MST), synthesizes H_2S in the presence of the substrate 3-mercaptopyruvate (3-MP). The immunohistochemistry analysis performed on human melanoma samples demonstrated that CSE expression was highest in primary tumors, decreased in the metastatic lesions and was almost silent in non-lymph node metastases. The primary role played by CSE was confirmed by the finding that the overexpression of CSE induced spontaneous apoptosis of human melanoma cells. The same effect was achieved using different H_2S donors, the most active of which was diallyl trisulfide (DATS). The main pro-apoptotic mechanisms involved were suppression of nuclear factor-κB activity and inhibition of AKT and extracellular signal-regulated kinase pathways. A proof of concept was obtained in vivo using a murine melanoma model. In fact, either L-cysteine, the CSE substrate, or DATS inhibited tumor growth in mice. In conclusion, we have determined that the L-cysteine/CSE/H_2S pathway is involved in melanoma progression.

Introduction

Melanoma is the deadliest form of skin cancer. Although early cutaneous melanoma is usually curable with surgery, distant metastatic melanoma is an aggressive cancer associated with a median survival time of 6 months. In 2013, almost 77 000 new melanoma diagnoses were expected and 9480 deaths were projected [National Cancer Institute; Melanoma Information Web Site. http://www.cancer.gov/cancertopics/types/melanoma (accessed 9 January 2014)]. Advances in understanding of melanoma immunobiology have resulted in two FDA-approved therapies for metastatic melanoma in 2011: vemurafenib, an inhibitor of mutant BRAF, an oncogene present in approximately 50% of melanomas, and ipilimumab, a monoclonal antibody that targets CTLA-4 (Hodi et al., 2010). However, the overall clinical benefit is limited to either small subgroups of patients who may be cured by immunotherapies or to a subset of patients with BRAF-mutant melanoma. Nevertheless, almost 50% of the BRAF-mutant melanoma patients develop resistance to the therapy that is molecularly targeted (Atefi et al., 2011; Johannessen et al., 2010; Nazarian et al., 2010; Poulikakos et al., 2011; Shi

Significance

The original aim of this study has been to identify new molecular targets in human metastatic melanoma. The main finding of our study was the demonstration of the involvement of the L-cysteine/cystathionine γ lyase/hydrogen sulfide pathway in human melanoma. Moreover, we provide fundamentals to exploit a possible therapeutic/diagnostic use of this pathway in this aggressive form of skin cancer.

© 2014 John Wiley & Sons A/S. Published by John Wiley & Sons Ltd

et al., 2012). More recently, two new drugs received FDA-approval: Dabrafenib (U.S. FDA. http://www.fda.gov/drugs/informationondrugs/approveddrugs/ucm354477htm), a BRAF inhibitor for melanoma targeted to tumors expressing the BRAF V600E gene mutation (Hauschild et al., 2012), and Trametinib (U.S. FDA. http://www.fda.gov/drugs/informationondrugs/approveddrugs/ucm354478), a MEK inhibitor, for melanoma targeted to tumors expressing BRAF V600E or V600K gene mutations (Flaherty et al., 2012).

In the last few years, numerous physiological and pathophysiological roles have been proposed for the gasotransmitter hydrogen sulfide (H_2S), along with a plethora of cellular and molecular targets (Wang, 2012). Cystathionine γ lyase (CSE) produces H_2S from L-cysteine alone in the presence of pyridoxal 5′-phosphate (PLP), whereas cystathionine β synthase (CBS) generates H_2S by condensation of L-cysteine and other thiols, such as L-homocysteine. Sequential reaction by the PLP-dependent enzyme, cysteine aminotransferase (CAT), and a PLP-independent enzyme, mercaptopyruvate sulfurtransferase (3-MST), has also been proposed as a potential H_2S-producing pathway. CAT forms 3-mercaptopyruvate (3MP) from L-cysteine and α-ketoglutarate (α-KG), and 3-MST subsequently catalyzes the formation of H_2S from 3MP in the presence of reducing agents.

A number of studies have investigated the role of H_2S in inducing cell death and evidence has been presented that this gas can exert both pro- and anti-apoptotic activity in cultured cells (Hu et al., 2007; Taniguchi et al., 2011). Recently, CBS has emerged as a potential therapeutic target in both colon cancer and ovarian cancer (Bhattacharyya et al., 2013; Szabo et al., 2013). The aim of our study was to evaluate the role of the metabolic H_2S pathway in human melanoma. To address this issue we: (i) determined the expression and localization of CSE, CBS and 3-MST in a panel of 102 human specimens including normal human epidermis, dysplastic nevi, primary lesions and melanoma metastases; (ii) evaluated, and differential modulated the expression of *CSE, CBS* and *3-MST* in human melanoma cells; (iii) investigated on the role of L-cysteine/CSE/H_2S pathway on human melanoma cell line survival and on tumor progression in vivo.

Results

CSE, CBS and 3-MST expression in human nevi

Expression of CSE, CBS and 3-MST was evaluated in six compound nevi, four junctional nevi and four dysplastic nevi. As shown in Table 1, all the dysplastic nevi (100%) were positive for CSE, negative for CBS and variable for 3-MST. Representative immunohistochemical-positive expressions of CSE, CBS and 3-MST in nevi and in melanomas, but not in lymph node metastases, are shown in Figure 1A.

Table 1. Contingency table of CSE, CBS and 3-MST expression in nevi. All specimens were analyzed by immunohistochemistry. The frequencies are indicated in rows in absolute values. The percentage is reported in brackets. 'pT', primary tumor; (–) no/low expression; (+) high expression

	CSE		CBS		3-MST	
Nevi	(–)	(+)	(–)	(+)	(–)	(+)
Compound	3 (50)	3 (50)	3 (50)	3 (50)	5 (83)	1 (17)
Junction	2 (50)	2 (50)	3 (75)	1 (25)	3 (75)	1 (25)
Dysplastic	0	4 (100)	4 (100)	0	1 (25)	3 (75)

CSE, CBS and 3-MST expression in human primitive melanoma and metastases

All specimens of primary melanoma analyzed by immunohistochemistry (n = 4) were positive for CSE expression (Table 2). CBS and 3-MST displayed a variable, but always very low, expression level in primary tumor (pT) (Table 2). A total of 72 melanoma metastases were analyzed. Metastases obtained were either lymph node metastases (n = 14) or tissue metastases (n = 58). Tissue metastases were distributed as follows: skin (22/58), lung (25/58), liver (6/58) and intestinal metastases (5/58). CSE-positive metastases were 39% (28/72); among these positive cases, 93% (26/28) were no lymph node metastases. CBS-positive metastases were 30% (22/72); among these positive cases 91% (20/22) were no lymph node metastases. 3-MST-positive metastases were 28% (20/72) none of which were lymph node metastases.

Expression of CSE, CBS and of 3-MST in human melanoma cell lines

To further address the role of the H_2S pathway in melanoma we performed a quantitative real-time PCR (qPCR) analysis of the expression levels of *CSE, CBS* and *3-MST* genes in normal human epidermal melanocytes (NHEM) and in a panel of four distinct human melanoma cell lines (A375, Sk-Mel-5, Sk-Mel-28 and PES 43). As shown in Figure 1B, the expression of the three genes was always very low in NHEM as opposed to melanoma cell lines, where *CSE, CBS* and *3-MST* were differentially expressed. In line with the immunohistochemistry data on humans, *CSE*, but not *CBS* or *3-MST*, was up-regulated in all the cell lines considered, although the difference was not statistically significant (Figure 1B).

Overexpression of CSE in A375 cells modifies cell proliferation

On the basis of the results obtained and to better elucidate the role of *CSE* in melanoma cells proliferation, we chose, as a tool, the cell line with the lowest *CSE* expression levels, the A375 melanoma cells. The *CSE*, *CBS* and *3-MST* genes were transiently overexpressed using a *hCSE* cDNA/pIRES2-EGFP, a *hCBS* cDNA/pCMV-SPORT6 or a *3-MST*/pCI-HA construct. Identical empty

© 2014 John Wiley & Sons A/S. Published by John Wiley & Sons Ltd

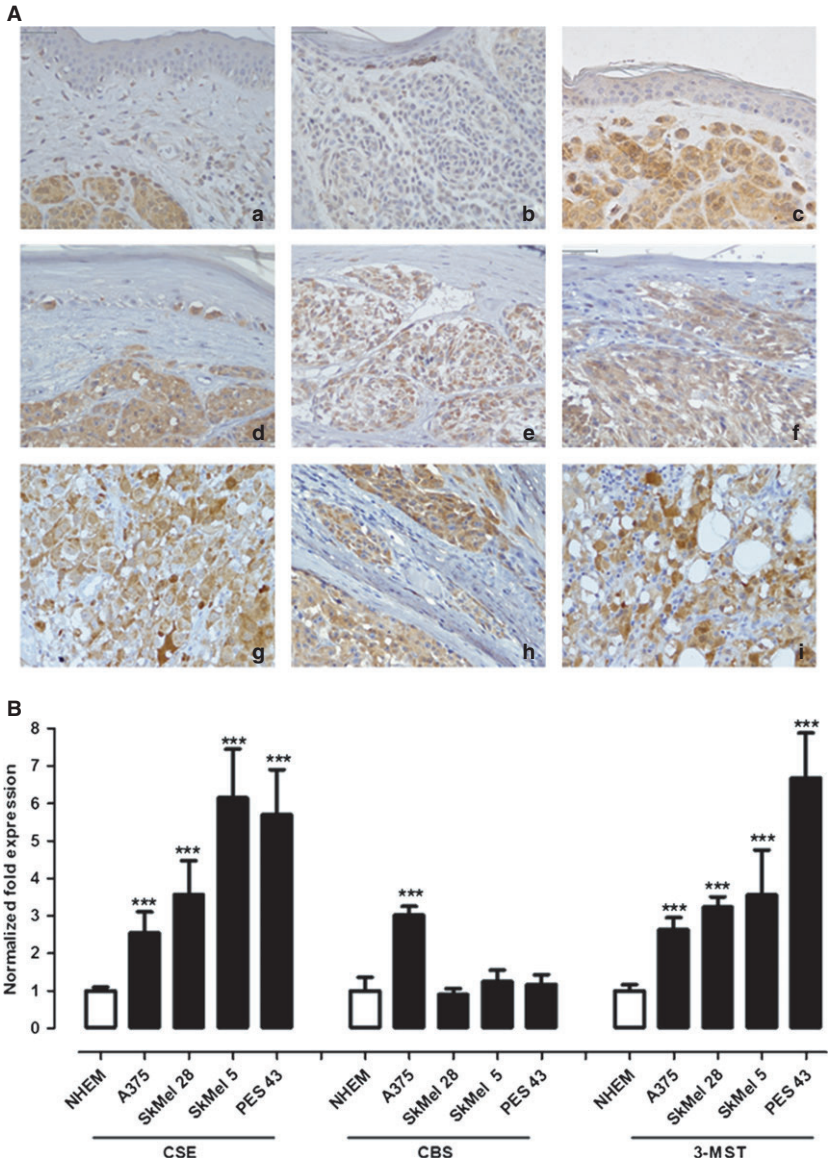

Figure 1. *CSE, CBS* and *3-MST* immunohistochemical and qPCR analysis. (A) Representative immunohistochemical positive expression of CSE, CBS and 3-MST in nevi (A, B, C; 40×); in melanomas (D, E, F; 40×); in no lymph nodes metastases (G,H, I; 40×). (B) mRNA expression levels of *CSE, CBS* and *3-MST* in NHEM, A375, Sk-Mel-5, Sk-Mel-28 and PES 43 cells evaluated by qPCR analysis. The expression of the three genes was very low in NHEM. In melanoma cell lines, *CSE*, *CBS* and *3-MST* were differentially expressed.. The results obtained by qPCR analysis are reported using the $2^{-\Delta Ct}$ formula. The housekeeping gene (ribosomal protein S16) was used as an internal control to normalize the ct values. Each column is the mean ± SEM of at least four independent determinations, each performed in quadruplicate. ***$P < 0.001$ versus NHEM.

vectors lacking a cDNA insert were used as control. Transfection of the cells with *CSE* cDNA, *CBS* cDNA, *3-MST* cDNA or with the empty vectors did not change the morphological characteristics of the cells. To determine whether the *CSE* overexpression affected the proliferation of human melanoma cell line, a 3-[4,5-dimethylthiazol-2-yl]-2,5-diphenyl tetrazolium bromide (MTT) proliferation assay was carried out. Proliferation of the *CSE*-overexpressing cells was inhibited by about 30% ($P < 0.001$) as compared with control cells (Figure 2A). Treatment with hemoglobin, a H_2S scavenger, reversed the anti-proliferative effect elicited by CSE overexpression, confirming the specificity of the effect. When A375 *CSE*-overexpressing cells were grown in the presence of L-cysteine (1 mM) the CSE substrate, the anti-proliferative effect was not significantly increased. *CBS* overexpression caused only a small inhibition ($P < 0.05$), which was not further increased when the cells were grown in the presence of L-cysteine. *3-MST* overexpression also slightly reduced cell proliferation and this effect was significantly increased ($P < 0.05$) in the presence of the enzyme substrate 3-MP (10 μM) (Figure 2). These data confirm a major role for CSE in melanoma and we therefore concentrated our attention on this enzyme.

© 2014 John Wiley & Sons A/S. Published by John Wiley & Sons Ltd

Table 2. Contingency table of CSE,CBS and 3-MST expression in primitive melanoma and metastases. All specimens were analyzed by immunohistochemistry. The frequencies are indicated in rows in absolute values. The percentage is reported in brackets. 'pT' primary tumor; (–) no/low expression; (+) high expression

	CSE		CBS		3-MST	
pT	(–)	(+)	(–)	(+)	(–)	(+)
1	0	4 (100)	3 (75)	1 (25)	3 (75)	1 (25
2	0	4 (100)	3 (75)	1 (25)	3 (75)	1 (25)
3	0	4 (100)	4 (100)	0	2 (50)	2 (50)
4	0	4 (100)	3 (75)	1 (25)	3 (75)	1 (25)
Metastasis sites						
No lymph node	32 (55.2)	26 (44.8)	38 (65.5)	20 (34.5)	38 (65.5)	20 (34.5)
Lymph node	12 (85.7)	2 (14.3)	12 (85.7)	2 (14.3)	14 (100)	0

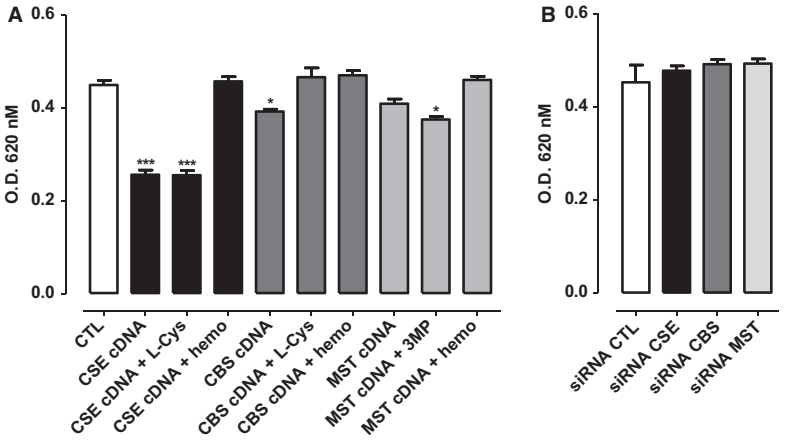

Figure 2. Overexpression and silencing of *CSE, CBS* and *3-MST* genes in A375 cells. (A) Overexpression of *CSE, CBS* and *3-MST* genes in A375 cells. *CSE* overexpression inhibited proliferation of human melanoma cells, as demonstrated by the MTT proliferation assay ***P < 0.001 versus Control (CTL). *CBS* overexpression only slightly (10%,*P < 0.05 versus CTL) inhibited proliferation of human melanoma cells, which was not further reduced by the addition of L-cysteine (1 mM). *3-MST* overexpression inhibited cell proliferation by about 7%, reaching 15% after the addition of the enzyme substrate 3-MP (10 μM) (*P < 0.05 versus CTL). Hemoglobin (10 μM), a H_2S scavenger, reversed the anti-proliferative effect induced by enzyme overexpression. Each column is the mean ± SEM of six independent experiments, each performed in quadruplicate. (B) Silencing of *CSE, CBS* and *3-MST* genes in A375 cells. Silencing of *CSE, CBS* and *3-MST* genes did not modify proliferation of human melanoma cells, as demonstrated by the MTT proliferation assay. Each column is the mean ± SEM of three independent experiments, each performed in quadruplicate.

We also performed silencing experiments on the A375 cell line. Cells were transiently transfected for 48 h with CSE Pre-designed siRNA, human CBS siRNA SMART pool or human 3-MST siRNA SMART pool. The negative control siRNA was used as internal control. As shown in Figure 2B, silencing of the genes did not modify cell proliferation.

Hydrogen sulfide donors inhibit human melanoma cell proliferation

To gain further insights into the role played by H_2S in human melanoma, we assessed the effect of several H_2S-donors on A375 cell proliferation (Table 3). All the compounds, but sodium hydrosulfide monohydrate (NaHS), inhibited the growth of A375 cells in a concentration-dependent manner (Table 3). Among all the H_2S donors tested, the most potent in inhibiting melanoma cell proliferation was DATS, with an IC_{50} of 89 μM. Similar results were obtained with all the other cell lines: Sk-Mel-5, Sk-Mel-28 and PES 43 (Table S1).

To better confirm that the anti-proliferative effect elicited by the H_2S-donors was not due to an artifact consequent to the hydrogen sulfide-induced reduction of mitochondrial respiration (MTT assay) we performed another proliferation assay, the 5-bromo-2′-deoxy-uridine assay. Results obtained with this assay show a greater anti-proliferative effect of DATS (100 μM; –73% P < 0.001) and of GYY4137 (1 mM; –39%, P < 0.001; Figure S1). On the basis of the results obtained with both assays, DATS was selected for all subsequent experiments together with GYY4137, another well characterized hydrogen sulfide donor (Lee et al., 2011).

Hydrogen sulfide donors cause cell cycle arrest and induce apoptosis of human melanoma cells

A375 human melanoma cells were treated with DATS and apoptosis was determined by annexin V/propidium iodide (PI) staining. This dual staining distinguishes between unaffected cells (unlabeled; quadrant 3,

 © 2014 John Wiley & Sons A/S. Published by John Wiley & Sons Ltd

Table 3. Effect of several H_2S-donors on A375 cell proliferation. Cell proliferation was measured using the MTT assay and expressed as OD values at 48 h. All the compounds used, but NaHS, inhibited the growth of A375 cells. Each experiment (n = 3) was run in quadruplicate

μM	CTL	NaHS	DATS	GYY4137	Thioglycine	Thiovaline
0	0.341 ± 0.02	–	–	–	–	–
3	–	0.350 ± 0.01	0.330 ± 0.01	–	–	–
10	–	0.357 ± 0.01	0.257 ± 0.01**	–	–	–
30	–	0.340 ± 0.005	0.240 ± 0.009***	–	–	–
100	–	0.365 ± 0.01	0.165 ± 0.02***	0.342 ± 0.002	0.343 ± 0.02	0.303 ± 0.02
300	–	0.351 ± 0.02	–	0.281 ± 0.003***	0.318 ± 0.02	0.250 ± 0.01*
1000	–	0.333 ± 0.01	–	0.244 ± 0.001***	0.210 ± 0.009**	0.200 ± 0.01***

*P < 0.05; **P < 0.01; ***P < 0.001 vs. CTL.

Figure 3A), early apoptotic cells (annexin V-positive; quadrant 4, Figure 3A), late apoptotic cells (annexin V-positive, PI-positive; quadrant 2, Figure 3A), and necrotic (PI-positive; quadrant 1; Figure 3A). Treatment of A375 cells for 3, 6, 24 and 48 h with DATS (100 μM) resulted in a time-dependent induction of apoptosis. In particular, at 48 h almost all cells (93%) exhibited markers of late apoptosis (Figure 3B). This effect was accompanied by a time-dependent cleavage of caspase 3 and of its substrate poly(adenosine diphosphate-ribose) polymerase (PARP) (Figure 3C). In addition, DATS treatment of A375 cells induced time-dependent accumulation of G_0/G_1-phase populations (Figure 3D,E). As expected, in DATS-treated cells, a reciprocal reduction of cell ratio in S and G_2/M phases was also observed (Figure 3D,E). Therefore, by donating hydrogen sulfide, DATS induces apoptosis and cell cycle arrest of human melanoma cells. To confirm that this effect was not a specific feature of DATS, the same study was repeated with GYY4137, another well characterized hydrogen sulfide donor with a different chemical structure. GYY4137 displayed a similar effect (Figure S2).

Hydrogen sulfide donors inhibit NF-κB activation and down-regulate NF-κB-dependent anti-apoptotic genes

Nuclear factor-κB (NF-κB) proteins are normally sequestered in the cytoplasm in an inactive form closely associated with the inhibitory protein inhibitor of kappa light chain gene enhancer in B cells-alpha (IκBα). Several reports have shown that in melanoma the constitutive activation of NF-κB confers tumor survival capacity and avoidance of apoptosis (Ueda and Richmond, 2006). Western blot analysis carried out on the cytosolic extracts obtained from A375 cells treated with DATS 100 μM for 15, 30 and 60 min showed an inhibition of IκBα degradation at the earliest time points (Figure 4A). To investigate the effect of hydrogen sulfide on NF-κB activity, A375 cells were treated with DATS (100 μM) at different time points (1, 3 and 6 h; Figure 4B). The A375 cell line was found to display a constitutively high NF-κB DNA binding activity, as compared with NHEM, which was reduced in a time-dependent manner by DATS. In fact, treatment with DATS (100 μM) for 3 and 6 h caused a significant (P < 0.001) inhibition of NF-κB-DNA binding activity by 30 and 76%, respectively (Figure 4C). The major NF-κB band in A375 cells consisted of the p50 and p65 subunits, as previously shown (Ianaro et al., 2009). Following on, we assessed the expression of three anti-apoptotic proteins, X-chromosome-linked inhibitor of apoptosis protein (XIAP), FLICE-inhibitory protein (c-FLIP) and B cell lymphoma gene-2 (Bcl-2), whose expression is modulated by the transcriptional activity of NF-κB. Western blot experiments showed that DATS markedly decreased the expression of all the anti-apoptotic genes considered (Figure 4D), confirming NF-κB involvement.

To verify that these effects were not a specific feature of DATS, the same experiments were carried out in the presence of GYY4137 and overlapping results were obtained (Figure S2).

Effect of hydrogen sulfide donors on MAPK/ERK and PI3/AKT pathways

Two of the most frequently deregulated pathways in melanoma are mitogen-activated protein kinase (MAPK)/ERK and phosphoinositide 3-kinase (PI3K)/AKT (Hodis et al., 2012). These two pathways play an important role in melanoma development and progression and are involved in the mechanism of resistance to targeted therapy (Flaherty et al., 2012). As shown in Figure 4E, both phospho-AKT (p-AKT) and phospho-ERK (p-ERK) band intensity was time-dependently reduced following treatment with DATS (100 μM). Similar results were obtained with GYY4137 (Figure S2). Thus, the pro-apoptotic effects of hydrogen sulfide on human melanoma involve a reduced activation of the AKT/p-AKT and ERK/p-ERK signaling pathways.

Hydrogen sulfide inhibits melanoma tumor in vivo in mice

To better elucidate the role of H_2S in melanoma development and progression, we used a well known murine model of melanoma (Berkelhammer et al., 1982), which is induced by subcutaneously injecting B16-F10 murine cells in C57BL/6 mice. L-Cysteine (600 mg/kg), the CSE substrate, was administered orally to mice. At day 14

© 2014 John Wiley & Sons A/S. Published by John Wiley & Sons Ltd

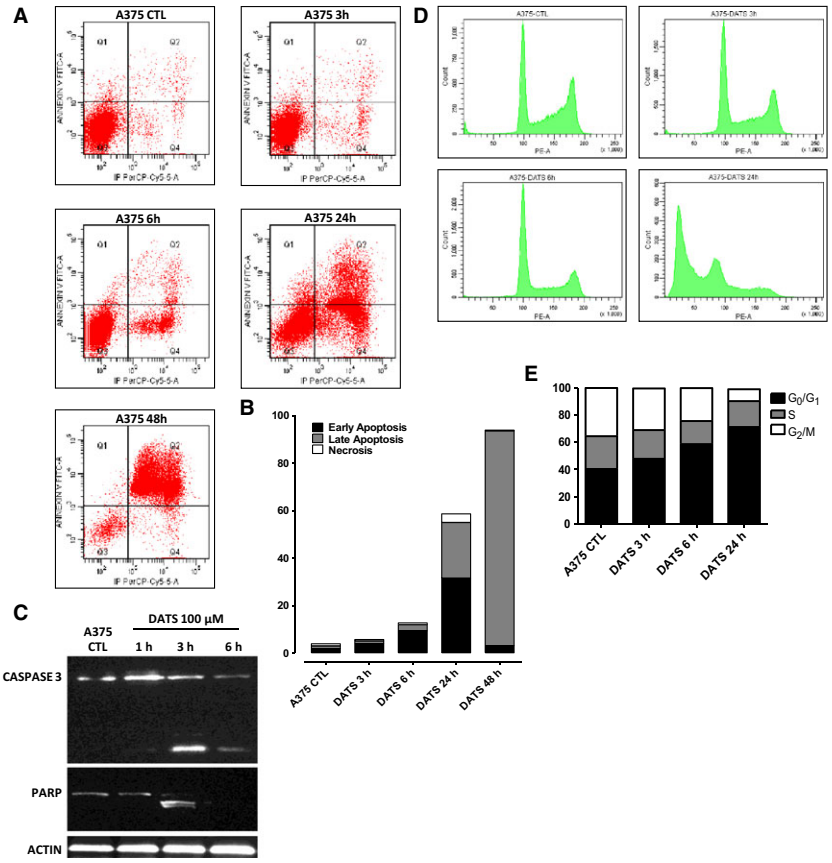

Figure 3. Induction of apoptosis and cell cycle arrest by the hydrogen sulfide-releasing donor DATS. (A) Cells were treated with DATS (100 μM) at different time points and apoptosis was determined by flow cytometry analysis. Apoptosis was determined by annexin V/propidium iodide (PI) staining, which detects the externalization of phosphatidylserine (PS). This dual staining distinguishes between unaffected cells (unlabeled; quadrant 3, Q3), early apoptotic cells (annexin V-positive; quadrant 4, Q4), late apoptotic cells (annexin V-positive, PI positive; quadrant 2, Q2), and necrotic (PI-positive; quadrant 1, Q1). Treatment of A375 cells for 3, 6, 24 and 48 h with DATS (100 μM) resulted in a time-dependent induction of apoptosis. (B) Quantitative analysis of DATS-induced A375 apoptosis at various time points showing that at 48 h almost all cells (93%) exhibit markers of late apoptosis. Experiments (n = 3) were run in triplicate. (C) Western blot analysis of caspase 3 and PARP in A375 whole-cell lysates. A375 cells were incubated with DATS 100 μM for 1, 3 and 6 h and a time-dependent cleavage of caspase 3 and of its substrate PARP was observed. Actin was detected as loading control. (D) Inhibition of cell cycle progression of human melanoma cells by DATS. DNA histogram shows the accumulation of G0/G1-phase cells induced by DATS in A375 cells. (E) Quantitative analysis of cell cycle distribution of vehicle treated or DATS-treated A375 cells at different time points. DATS treatment of A375 cells induced a time-dependent accumulation of G_0/G_1-phase populations (column black area). As expected, in DATS-treated cells, a reciprocal reduction of cell ratio in S (column gray area) and in G_2/M-phases (column white area) was also observed. Experiments (n = 3) were run in triplicate.

after tumor implantation, a 51% reduction in tumor volume was observed in L-cysteine-treated mice (0.170 ± 0.03 cm^3 mean tumor volume versus control mice 0.347 ± 0.03 cm^3 mean tumor volume, $P < 0.001$) (Figure 5A). The protective effect of L-cysteine was abolished following co-administration to mice of DL-propargylglycine (PAG; 10 mg/kg), a selective CSE inhibitor (Sun et al., 2009) (0.353 ± 0.04 cm^3 mean tumor volume, $P < 0.001$ versus L-cysteine alone; Figure 5A). The tumor growth inhibition obtained by the endogenous-CSE-derived hydrogen sulfide was mimicked by the exogenous hydrogen sulfide delivered to mice following administration of DATS. In fact, DATS (50 mg/kg) significantly ($P < 0.001$) inhibited tumor growth by 67% (0.07 ± 0.001 cm^3 mean tumor volume) as compared with control mice (0.210 ± 0.004 cm^3 mean tumor volume) (Figure 5B).

Discussion

It is becoming clear that melanoma constitutes a heterogeneous group of tumors with different patterns of oncogenic mutation, overexpression and genomic amplification. The interactions between the various signaling molecules involved in melanoma progression are best viewed as a series of links between a number of interconnected nodes. One feature of these networks is their robustness, demonstrated clinically by the ability to develop resistance to current therapies. It is known that about 50% of patients treated with BRAF or MEK

© 2014 John Wiley & Sons A/S. Published by John Wiley & Sons Ltd

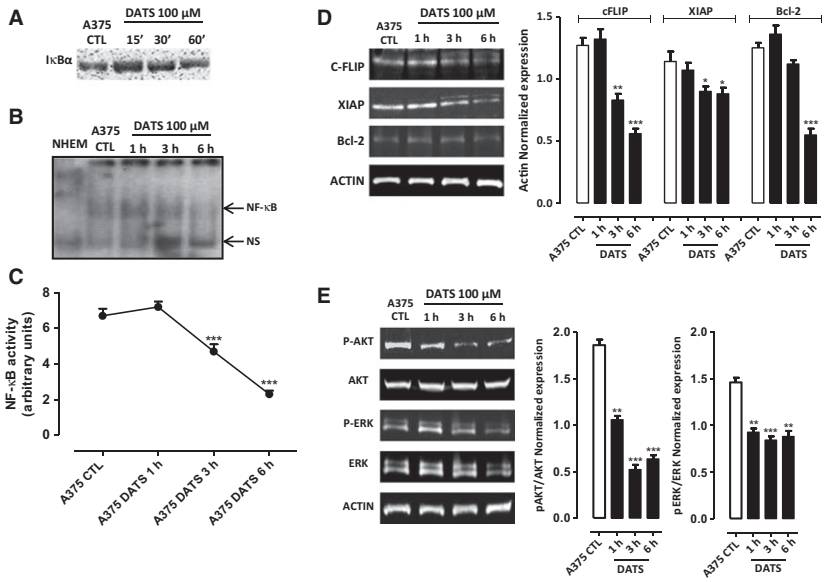

Figure 4. Melanoma cells constitutively express activated NF-κB to promote anti-apoptotic and pro-survival signaling. (A) Western blot analysis carried out on the cytosolic extracts obtained from A375 cells treated with DATS 100 μM for 15, 30 and 60 min shows an inhibition of IκBα degradation at the earlier time points. (B) Nuclear extracts from control-treated and DATS-treated A375 cells collected at 1, 3 and 6 h were analyzed by EMSA for NF-κB activation. The A375 cell line displayed a constitutively high NF-κB DNA binding activity, as compared with NHEM, that was reduced in a time-dependent manner by DATS. These data are expressed as arbitrary units and shown in panel C (***P < 0.001 versus CTL). (D) Western blot analysis and relative densitometry of c-FLIP, XIAP and Bcl-2 carried out on A375 cells treated with DATS 100 μM for 1, 3 and 6 h. The hydrogen sulfide donor markedly decreased the expression of all the anti-apoptotic genes analyzed; ***P < 0.001; **P < 0.01; *P < 0.05 versus CTL. Actin was detected as a loading control. (E) Western blot analysis and relative densitometry of phospho- and total AKT and ERK in A375 cells treated with DATS 100 μM for 1, 3 and 6. Both p-AKT and p-ERK band intensities were time-dependently reduced following treatment with DATS (100 μM); ***P < 0.001; **P < 0.01 versus CTL. Actin was detected as a loading control. Experiments (n = 3) were run in triplicate.

inhibitors have disease progression within 6–7 months after the initiation of treatment. Therefore, it is critical to identify other important potential targets in melanoma development and progression that are amenable to pharmacological inhibition. It has been shown previously that CSE is expressed in melanoma cell lines (Jurkowska et al., 2011) but the role of the hydrogen sulfide pathway has never been investigated. Conversely, a role for this pathway has been proposed in colon and ovarian cancer, where it is mainly driven by CBS (Bhattacharyya et al., 2013; Szabo et al., 2013). To evaluate the involvement of the hydrogen sulfide pathway in melanoma, we analyzed the expression of CSE, CBS and 3-MST in human tissue samples. The immunohistochemical analysis performed on more than 100 human samples demonstrated that CSE expression increased from nevi to primary melanoma, decreased in tissue metastases and was absent in lymph node metastases. Conversely, analysis of CBS expression revealed that this enzyme was absent in dysplastic nevi. Positive CBS expression was found in only 25% of the primary melanomas analyzed. Therefore, as opposed to other types of cancer (Bhattacharyya et al., 2013; Szabo et al., 2013) CBS does not appear to play an important role in human melanoma. 3-MST expression was always extremely variable in the human specimens analyzed (from nevi to metastasis). The finding that CSE expression is higher in primary melanoma than in distant metastatic melanoma, suggests the involvement of this pathway in the progression of melanoma. To obtain further insights into the role of the hydrogen sulfide pathway, we analyzed several melanoma cell lines, widely used in the relevant literature, for the purpose of selecting a cell line suitable to perform a molecular modulation study. All the melanoma cells selected expressed *CSE, CBS* and *3-MST* differently. Whereas *CSE* expression was higher in all melanoma cells analyzed as compared with NHEM, *CBS* expression was enhanced in A375 cells only, and *3-MST* showed a variable pattern of expression among all cell lines. Thus, to further confirm the primary role of *CSE* versus *CBS* and *3-MST*, we selected as a tool the A375 cell line. Overexpression of *CSE* in A375 inhibited cellular proliferation (50%). Treatment with hemoglobin, a hydrogen sulfide scavenger, reversed the anti-proliferative effect elicited by *CSE* overexpression, confirming the specificity of the effect. *CBS* overexpression caused only a small inhibition of cell proliferation (about 10%) that was not further increased by the addition of L-cysteine. The same magnitude of effect, about 8%, was observed following *3-MST* overexpression. Addition of 3-MP, the enzyme substrate, increased the anti-proliferative effect up to 15%. These data support our hypothesis that CSE-derived hydrogen sulfide plays a major role in melanoma.

© 2014 John Wiley & Sons A/S. Published by John Wiley & Sons Ltd

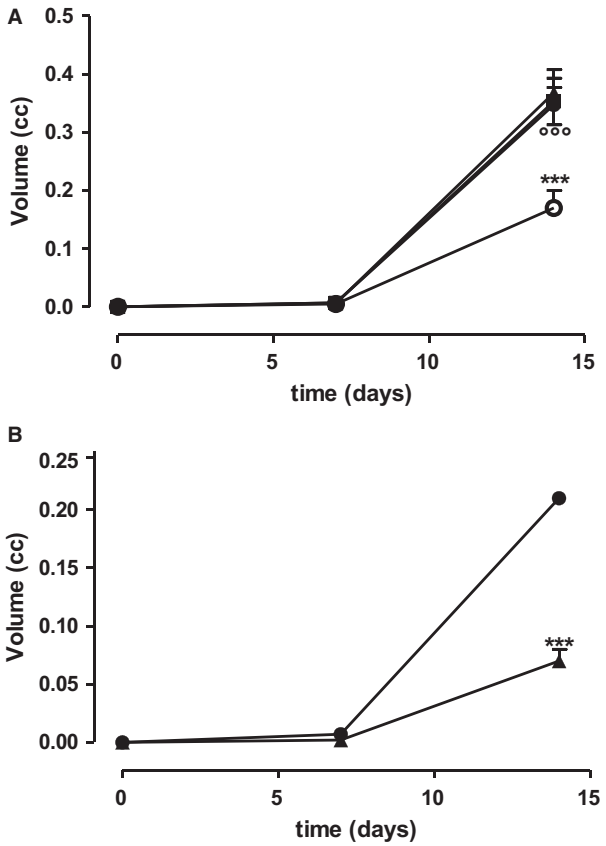

Figure 5. Hydrogen sulfide inhibits tumor growth in vivo. (A) L-cysteine (L-Cys 600 mg/kg,○), PAG (10 mg/kg, ▲) or a combination of drugs (L-Cys+PAG, ■) were given orally to mice; control mice (●) received vehicle only. Tumor volume was monitored on the indicated days. The average tumor volume with standard error is plotted against the days after tumor implant. L-Cysteine significantly reduced tumor volume (***P < 0.001 versus control, n = 8; day 14); the inhibitory effect of L-cysteine was abolished by PAG (°°°P < 0.001 versus L-Cys, n = 8). (B) The H_2S-donor DATS (50 mg/kg, ▲) significantly inhibited tumor growth (***P < 0.001 versus control, n = 8).

Our results are in line with a previous study showing that overexpression of *CSE* in HEK-293 results in the inhibition of cellular proliferation and DNA synthesis (Yang et al., 2004). On the other hand, the silencing of all three enzymes did not modify cellular proliferation, implying that reduction of the basal endogenous level of H_2S production does not affect cell survival, or a compensatory mechanism may intervene.

It has been shown that activation of the H_2S pathway can exert both pro- and anti-apoptotic activity in cultured cells (Hu et al., 2007; Taniguchi et al., 2011). These studies have been conducted on immortalized cell lines mainly using NaHS as the exogenous source of hydrogen sulfide. The use of NaHS as donor has two main drawbacks: (i) the fast kinetics of hydrogen sulfide release and (ii) the high concentrations used, often in the mM range. These two issues suggest that discrepancies (e.g. pro- and anti-apoptotic effect) may lie in the choice of the hydrogen sulfide donors used. Sulfide salts such as NaHS and sodium sulfide (Na_2S) on addition of water generate a burst of hydrogen sulfide within a short period as opposed to the organic donors (Lee et al., 2011). Since cell culture takes place over a period of hours or days, it is likely that little, if any, hydrogen sulfide is present in medium within a short time of adding either NaHS or Na_2S. It is therefore necessary to perform repeated challenge or to use high (mM) doses. In a recent comparative study showing differences between fast (NaHS) and slow-release (GYY4137) H_2S donors, it was demonstrated that only GYY4137 caused a concentration-dependent killing of several human cancer cell lines (Lee et al., 2011). Therefore, in our study we used both fast (NaHS) and slow releasers (DATS, GYY4137, thioglycine and L-thiovaline). All the compounds used, except NaHS, although with different IC_{50}, inhibited cellular proliferation. The most active among the H_2S-donors tested was DATS and it was selected for the molecular studies since its hydrogen sulfide-delivering property has been well characterized (Benavides et al., 2007). Cytofluorimetric studies demonstrated that the anti-proliferative effect of DATS was due to its ability to induce apoptosis and cell cycle arrest. Caspase-3 is the main 'effector' caspase in the apoptotic pathway, which acts through cleavage of its well-known substrate PARP. The finding that DATS induces caspase 3 activation further confirmed that H_2S triggers apoptosis. Many chemotherapeutic agents cause cell-cycle arrest but not apoptosis and this is one of the mechanisms leading to chemoresistance. In fact, growth arrest allows cells to repair their DNA and limits the efficacy of chemotherapy. Thus, by overriding tumor resistance to apoptosis, agents such as hydrogen sulfide donors are of great potential value. The apoptotic machinery can be controlled, at least in part, by NF-κB, which regulates transcription of the Bcl-2 family members (Ben-Neriah and Karin, 2011). Constitutive activation of NF-κB and AKT has been described in melanoma (Kantrow et al., 2007). Here we show that hydrogen sulfide donors inhibit IκBα degradation and this effect was associated to the inhibition of NF-κB nuclear translocation and activation. The issue of whether exogenous hydrogen sulfide inhibits (Fan et al., 2013; Guo et al., 2013; Li et al., 2013; Oh et al., 2006; Pan et al., 2011, 2012; Shankar et al., 2008; Sivarajah et al., 2009; Tripatara et al., 2008) or activates (Sen et al., 2012) NF-κB signaling pathway has been a matter of debate. In fact, in the relevant literature diametrically opposite views exist on the roles of this gas in NF-κB activation. However, the different experimental settings (in vitro versus in vivo) coupled to the different stimuli as well as to the protocols used do not allow a clear conclusion to be drawn. It has been shown that the slow-releasing hydrogen sulfide donor derivatives of diclofenac (Frantzias et al., 2012; Li et al., 2007; Wallace et al., 2007) and aspirin (Chattopadhyay et al., 2012) also inhibit NF-κB activation. In addition, it

 © 2014 John Wiley & Sons A/S. Published by John Wiley & Sons Ltd

has recently been shown that hydrogen sulfide inhibits NF-κB activation in ox LDL-induced macrophage inflammation through both sulfhydration of free thiol group on cysteine 38 in p65 subunit and inhibition of IκBα degradation (Du et al., 2014). In our study and experimental settings we found that hydrogen sulfide inhibits IκBα degradation, leading to inhibition of NF-κB nuclear translocation. Thus our results are in line with the inhibitory effect of hydrogen sulfide on NF-κB activation (Fan et al., 2013; Guo et al., 2013; Li et al., 2013; Oh et al., 2006; Pan et al., 2011, 2012; Shankar et al., 2008; Sivarajah et al., 2009; Tripatara et al., 2008). The fact that NF-κB is inhibited by H_2S is also supported by the finding that treatment with hydrogen sulfide donors greatly decreased the expression of the anti-apoptotic proteins c-FLIP, XIAP and Bcl-2. Indeed, these proteins are known to be transcriptionally regulated by NF-κB (Ben-Neriah and Karin, 2011).

To better define the mechanism by which this critical effect is achieved, we investigated on the possible involvement of the MAPK/ERK and the PI3K/AKT pathways. These pathways are the two most frequently deregulated pathways in melanoma and are also involved in primary and secondary resistance to BRAF inhibitors (Atefi et al., 2011; Hodis et al., 2012; Johannessen et al., 2010; Nazarian et al., 2010; Poulikakos et al., 2011; Shi et al., 2012). Both DATS and GYY4137 inhibited the phosphorylation of AKT and ERK. Therefore, feeding hydrogen sulfide to melanoma cells leads to down-regulation of the two main pathways involved in melanoma resistance. Our results are in agreement with other reports showing that exogenous hydrogen sulfide inhibits the activation of both AKT and MAPK pathways (Guo et al., 2013; Shankar et al., 2008; Tripatara et al., 2008).

Starting from evidence that CSE is expressed in human melanoma, our study demonstrates that in A375 cells, CSE but not CBS overexpression induces spontaneous apoptosis and exogenous hydrogen sulfide induces apoptosis. This apoptotic effect involves: (i) the suppression of pro-survival pathways associated to NF-κB transcription activity as demonstrated by the decreased expression of c-FLIP, XIAP and Bcl-2 and (ii) the inhibition of the activation of AKT and ERK1/2 downstream signaling pathways. To support these results, we developed a translational in vivo pre-clinical approach. For this purpose we used an animal model that recapitulates human cutaneous melanoma progression, the spontaneous C57BL/6-derived B16 melanoma cell line (Berkelhammer et al., 1982) because it is well-established and is a widely used tumor model. We demonstrated that L-cysteine, the natural substrate of CSE, significantly reduced tumor volume and this effect was completely abolished by PAG, the selective CSE inhibitor. To further support our in vitro findings we also used DATS in vivo. DATS significantly inhibited tumor volume development. These data, together with previous evidence, confirm the involvement of hydrogen sulfide in melanoma progression.

In conclusion, we have demonstrated, starting from the evidence acquired with human specimens, the involvement of the L-cysteine/CSE/hydrogen sulfide pathway in human melanoma. Our study provides proof-of-principle toward establishing this pathway as a potential therapeutic target in melanoma.

Methods

Cell culture and reagents

NHEM was purchased from Lonza (Walkersville, MD, USA) and grown in melanocyte growth medium 2 (Lonza). The melanoma cell lines B16/F10, Sk-Mel-5 and Sk-Mel-28 were purchased from IRCCS AOU San Martino – IST (Genua, Italy), A375 from Sigma–Aldrich (Milan, Italy). The cell lines were cultured in Dulbecco's modified Eagle's medium (DMEM) containing 10% fetal bovine serum, 2 mmol/l L-glutamine, 100 μmol/l nonessential amino acids, penicillin (100 U/ml), streptomycin (100 μg/ml) and 1 mmol/l sodium pyruvate (all from Sigma–Aldrich). Cells were grown at 37°C in a humidified incubator under 5% CO_2. The cell line PES 43 was isolated from a lung metastases of a patient from the National Cancer Institute, G. Pascale Foundation (Scala et al., 2006), and cultured in Iscove's modified Dulbecco's medium (Cambrex Bioscience, Verviers, Belgium) supplemented with heat-inactivated 10% fetal bovine serum, penicillin and streptomycin (100 units/ml each). DATS (LKT Laboratories) was diluted in DMSO to produce a stock solution of 10 mM for in vitro experiments; GYY4137 (Cayman Chemical, Ann Arbor, MI, USA) was solubilized in PBS; PAG, 3-MP and NaHS (Sigma–Aldrich) were solubilized in H_2O; thioglycine and L-thiovaline, a kind gift of Prof. Andreas Papapetropoulos, were solubilized in PBS.

Preparation of cellular extracts and Western blot analysis

A375 cells were treated with DATS 100 μM for 1, 3 and 6 h or with GYY4137 1 mM for 3, 6 and 24 h. Whole-cell or nuclear extracts were prepared as previously described (Ialenti et al., 2005). The protein concentration was measured by the Bradford method (Bio-Rad, Milan, Italy). Equal amounts of protein (40 μg/sample) from whole or nuclear cell extracts were separated by sodium dodecylsulfate polyacrylamide gel electrophoresis (SDS-PAGE) and blotted onto a nitrocellulose membranes (Trans-Blot Turbo Transfer Starter System, Bio-Rad). The membranes were blocked for 2 h in 5% low-fat milk in PBS with 0.1% Tween 20 (PBST) at room temperature. Then the filters were incubated with the following primary antibodies: IκBα (sc-1643 Santa Cruz Biotechnology, Santa Cruz, CA, USA; diluted 1 : 200); Bcl-2 (2876, Cell Signaling, Beverly, MA, USA; diluted 1 : 1000); caspase 3 (9662, Cell Signaling; diluted 1 : 1000); PARP (9542, Cell Signaling; diluted 1 : 1000); p44/42 MAPK (Erk1/2) (9102, Cell Signaling; diluted 1 : 1000); phospho-p44/42 Erk MAPK (Erk1/2, Thr202/Tyr204) XP (4370, Cell Signaling; diluted 1: 2000); AKT (9272, Cell Signaling; diluted 1 : 1000); phospho-AKT (Ser473) XP (4060, Cell Signaling; diluted 1 : 2000); c-FLIP (06-864, Millipore; diluted 1 μg/ml); XIAP (R&D Systems, Minneapolis, MN, USA; 1 μg/ml); NF-κB p65 (F-6) (sc-8008 Santa Cruz Biotechnology; diluted 1 : 200); β-actin (Santa Cruz Biotechnology; diluted 1 : 1000) overnight at 4°C. The membranes were washed three times with PBST and then incubated with horseradish peroxidase-conjugated antibodies (Santa Cruz Biotechnology; diluted 1 : 2000) for 2 h at room temperature. The immune complexes were visualized by the ECL chemiluminescence method and acquired by the Image Quant 400 system (GE Healthcare).

© 2014 John Wiley & Sons A/S. Published by John Wiley & Sons Ltd

Patients and specimens

In all, 102 patients of the National Cancer Institute 'Giovanni Pascale' of Naples have been included in this study from 2004 to 2012. All patients were caucasians, and all gave their written informed consent according to the institutional regulations. This study was approved by the ethics committee of the National Cancer Institute 'G. Pascale'.

Immunohistochemistry analysis

Tissue samples were retrieved from the paraffin blocks of the National Cancer Institute of Naples archives. Hematoxylin & eosin staining of a 4-μm section was used to verify all samples. Immunohistochemical analysis was performed on 4-μm sections from formalin-fixed, paraffin-embedded tissues in order to evaluate the expression of CSE and CBS. Negative control slides without primary antibody were included for each staining. Paraffin slides were deparaffinized in xylene and rehydrated through graded alcohols. Antigen retrieval was performed with slides heated in 0.01 M citrate buffer (pH 6.0) for CSE antibody and 1 mM EDTA buffer, pH 8.0 for CBS and 3-MST antibodies, in a bath for 20 min at 97°C. After antigen retrieval, the slides were allowed to cool. The slides were rinsed with TBS and the endogenous peroxidase inactivated with 3% hydrogen peroxide. After protein block (BSA 5% in PBS 1 ×), every slide was incubated with specific primary antibody: anti-CSE (clone 2E12-1C10, mouse, 1 : 1200, Novus Biologicals, Ltd, Cambridge, UK; anti CBS (clone H-300, rabbit, 1 : 500, Santa Cruz Biotechnology) anti 3-MST (clone NBP1-54734, rabbit 1 : 500, Novus Biologicals). The sections were rinsed in TBS and incubated for 20 min with Novocastra biotinylated secondary antibody (RE7103), a biotin-conjugated secondary antibody formulation that recognizes mouse and rabbit immunoglobulins. Then the sections were rinsed in TBS and incubated for 20 min with Novocastra streptavidin-HRP (RE7104). Finally, peroxidase reactivity was visualized using 3,3′-diaminobenzidine (DAB) and the sections counterstained with hematoxylin and mounted. Results were interpreted using a light microscope. CSE, CBS and 3-MST expression was evaluated in stained tissue sections by two pathologists (G.B, A.A.) in a blinded manner. In each sample the number of positive cells was evaluated in 10 non-overlapping fields using ×400 magnification. Data are expressed as the percentage of positive cancer cells over the total number of cancer cells. The obtained median value was used as cut off for that specific marker (CSE, CBS, 3-MST). Therefore in order to be defined as negative, a sample has to be equal or below the median value.

RNA purification and qPCR

Total RNA was isolated from cells using the TRI-Reagent (Sigma–Aldrich, Milan, Italy) according to the manufacturer's instructions, followed by spectrophotometric quantization. Final preparation of RNA was considered DNA- and protein-free if the ratio between readings at 260/280 nm was ≥1.7. Isolated mRNA was reverse-transcribed by iScript Reverse Transcription Supermix for RT-qPCR (Bio-Rad, Milan, Italy). qPCR was carried out in CFX384 real-time PCR detection system (Bio-Rad) with specific primers using SYBR Green master mix kit (Bio-Rad). Samples were amplified simultaneously in triplicate in a one-assay run with a non-template control blank for each primer pair to control for contamination or primer-dimers formation, and the ct value for each experimental group was determined. The housekeeping gene (ribosomal protein S16) was used as an internal control to normalize the ct values, using the $2^{-\Delta Ct}$ formula.

Transfection

A375 cells were seeded onto 96-well plates (2×10^3 cell/well) and transfected the next day with the human *CSE*/pIRES-EGFP, the human *CBS* cDNA/pCMV-SPORT6 or the human *3-MST*/pCI-HA using Lipofectamine 2000 (Life Technologies, Milan, Italy). Forty-eight hours after transfection, cell proliferation was evaluated by MTT assay (see Proliferation assays). Western blot analysis of CSE, CBS and 3-MST expression was carried out on whole cell extracts to confirm effective gene overexpression (anti-CSE, clone 2E12-1C10, mouse, 1: 500, Novus Biologicals, Ltd; anti-CBS, clone H-300, rabbit, 1 : 500, Santa Cruz Biotechnology); anti-3-MST (clone NBP1-54734, rabbit 1 : 500, Novus Biologicals). For the silencing experiments, A375 cells were seeded onto 96-well plates (2 × 103 cell/well) and transfected the next day, according to the manufacturer's instructions, with CSE Silencer® Select Pre-designed siRNA (Ambion, Carlsbad, CA, USA) (sense strand 5′-CUAUGUAUUCUGCAACAAtt-3′, antisense strand, 5′- UUUGUUGCAGAAUACAUAGaa-3′); human 3-MST siRNA SMART pool siGENOME (Thermo-Fisher Scientific, Hudson, NH, USA) (GGAGAAGAGCCCUGAGGAG, CCGCCUUCA UCAAGACCUA, CCACCCACGUCGUGAUCUA, AGAAAGUGGACCU GUCUAA); human CBS siRNA SMART pool siGENOME (GGAAGAA GUUCGGCCUGAA, GGACGGUGGUGGACAAGUG, CACCACCGCU-GAUGAGAUC, AGACGGAGCAGACAACCUA). Forty-eight hours after transfection, cell proliferation was evaluated by MTT assay (see Proliferation assays).

Proliferation assays

Cell proliferation was measured by the MTT assay as previously described (Panza et al., 2011) or by the 5-bromo-2′-deoxy-uridine assay following the manufacturer's instructions (Roche, Milan, Italy). Briefly, for the MTT assay the human melanoma cells (A375, Sk-Mel-5, Sk-Mel-28 and PES 43) and the NHEM cells were seeded onto 96-well plates (2×10^3 cells/well) a day earlier and successively treated with vehicle or various concentrations of different H_2S-releasing compounds for 24, 48 and 72 h before adding 25 μl MTT (Sigma–Aldrich; 5 mg/ml in saline). Cells were then incubated for an additional 3 h at 37°C. After this time interval, cells were lysed and dark blue crystals were solubilized with a solution containing 50% N, N-dimethyl formamide and 20% sodium dodecylsulfate with an adjusted pH of 4.5. The optical density of each well was measured with a microplate spectrophotometer (TitertekMultiskan MCC/340), equipped with a 620-nm filter. None of the compounds tested under the same experimental conditions had a cytotoxic effect on NHEM.

Flow cytometry

Apoptosis was detected with an annexin V-FITC (BD Pharmingen, San Diego, CA, USA) according to manufacturer's instructions. A375 cells were seeded in 35-mm culture dishes and allowed to attach overnight. The cells were treated with DATS (100 μM) for 3, 6, 24 and 48 h, collected, and washed twice with PBS. Samples were then taken to determine baseline and drug-induced apoptosis by Annexin V-FITC/propidium iodide (PI) (Beckman Coulter, Brea, CA, USA) double staining or PI staining and flow cytometry analysis using a FACSCanto II 6-color flow cytometer (Becton Biosciences, San Jose, CA, USA), as described previously (Ianaro et al., 2009). To detect early and late apoptosis, both adherent and floating cells were harvested together and resuspended in annexin V binding buffer (10 mM HEPES/NaOH pH 7.4, 140 mM NaCl, 2.5 mM $CaCl_2$) at a concentration of 10^6 cells/ml. Subsequently, 5 μl of FITC-conjugated Annexin V and 5 μl of PI were added to 100 μl of the cell suspension (10^5 cells). The cells were incubated for 15 min at room temperature in the dark. Finally, 400 μl of annexin V-binding buffer was added to each tube. A minimum of 50 000 events for each sample were collected and data were analyzed using FACSDIVA software (Becton Biosciences).

Cell cycle

Cells were plated in six-well plates at a density of 5×10^5 cells/well. Cells were then treated with DATS 100 μM for 3, 6 and 24 h. Cells

 © 2014 John Wiley & Sons A/S. Published by John Wiley & Sons Ltd

were collected, washed twice with ice-cold PBS buffer (pH 7.2–7.4), fixed with 70% alcohol overnight and stained with PI (1 mg/ml) in the presence RNAse A (1 mg/ml) for at least 30 min prior to analysis by flow cytometry. The flow-cytometric analysis was performed using a FACSCanto II and the cycle analysis was performed with the MODFIT LT software (Verity Software House).

Electrophoretic mobility shift assay (EMSA)

Aliquots of total extracts (12 μg protein/sample) in 0.1% Triton X-100 lysis buffer were incubated with ^{32}P-labeled κB DNA probes in binding buffer for 30 min, as previously described (Panza et al., 2011). DNA-protein complexes were analyzed using non-denaturing 4% polyacrylamide gel electrophoresis. Quantitative evaluation of NF-κB-κB complex formation was done using a Typhoon-8600 imager (Molecular Dynamics Phoshor-Imager, MDP, Amersham Biosciences, Piscataway, NJ, USA) and IMAGEQUANT software (Amersham Biosciences) (MDP analysis). For control of equal loading, NF-κB values were normalized to the level of the nonspecific protein-DNA complex in the same lane.

In vivo experiments

Animals

Animal care was in accordance with Italian and European regulations on the protection of animals used for experimental and other scientific purposes. Mice were observed daily and humanely euthanized by CO_2 inhalation if a solitary subcutaneous tumor exceeded 1.5 cm in diameter or mice showed signs referable to metastatic cancer. All efforts were made to minimize suffering. Female C57BL/6 mice (18–20 g) were from Charles River Laboratories, Inc. Mice were housed at the Animal Research Facility of the Department of Pharmacy of the University of Naples Federico II.

Induction of subcutaneous B16 lesions

Mice were subcutaneously (s.c.) injected in the right flank with B16-F10 cells (1×10^5/0.1 ml). When tumors reached an average diameter of 2–4 mm, L-cysteine (600 mg/kg), DATS (50 mg/kg) or a combination of L-cysteine + PAG (10 mg/kg) was given orally. Control mice received only vehicle. Tumor size was measured using a digital caliper, and tumor volume was calculated using the following equation: tumor volume = $\pi/6(D1 \times D2 \times D3)$ where D1 = length; D2 = width; D3 = height and expressed as cm^3.

Statistical analysis

Data from all in vivo experiments are reported as mean ± SEM unless otherwise noted. Data were analyzed and presented using GRAPHPAD PRISM software (GraphPad). Significance was determined using Student's 2-tailed t-test. Results were considered significant at P values less than 0.05 and are labeled with a single asterisk. In addition, P values less than 0.01 and 0.001 are designated with double and triple asterisks, respectively.

Acknowledgements

Funding of this research was provided by P.O.R. Campania FSE 2007–2013, Progetto CREME, CUP B25B09000050007; by Italian Government grants (PRIN 2010-2011; FIRB 2012).

Conflict of interest

No conflict of interest declared.

References

Atefi, M., von Euw, E., Attar, N. et al. (2011). Reversing melanoma cross-resistance to BRAF and MEK inhibitors by co-targeting the AKT/mTOR pathway. PLoS ONE *6*, e28973.

Benavides, G.A., Squadrito, G.L., Mills, R.W., Patel, H.D., Isbell, T.S., Patel, R.P., Darley-Usmar, V.M., Doeller, J.E., and Kraus, D.W. (2007). Hydrogen sulfide mediates the vasoactivity of garlic. Proc. Natl Acad. Sci. USA *104*, 17977–17982.

Ben-Neriah, Y., and Karin, M. (2011). Inflammation meets cancer, with NF-kB as the matchmaker. Nat. Immunol. *12*, 715–723.

Berkelhammer, J., Oxenhandler, R.W., Hook, R.R. Jr, and Hennessy, J.M. (1982). Development of a new melanoma model in C57BL/6 mice. Cancer Res. *42*, 3157–3163.

Bhattacharyya, S., Saha, S., Giri, K. et al. (2013). Cystathionine beta-synthase (CBS) contributes to advanced ovarian cancer progression and drug resistance. PLoS ONE *8*, e79167.

Chattopadhyay, M., Kodela, R., Nath, N., Barsegian, A., Boring, D., and Kashfi, K. (2012). Hydrogen sulfide-releasing aspirin suppresses NF-kB signaling in estrogen receptor negative breast cancer cells in vitro and in vivo. Biochem. Pharmacol. *83*, 723–732.

Du, J., Huang, Y., Yan, H. et al. (2014). Hydrogen sulfide suppresses oxidized low-density lipoprotein (ox-LDL)-stimulated monocyte chemoattractant protein 1 generation from macrophages via the nuclear factor kB (NF-kB) pathway. J. Biol. Chem. *289*, 9741–9753.

Fan, H., Guo, Y., Liang, X., Yuan, Y., Qi, X., Wang, M., Ma, J., and Zhou, H. (2013). Hydrogen sulfide protects against amyloid beta-peptide induced neuronal injury via attenuating inflammatory responses in a rat model. J. Biomed. Res. *27*, 296–304.

Flaherty, K.T., Infante, J.R., Daud, A. et al. (2012). Combined BRAF and MEK inhibition in melanoma with BRAF V600 mutations. N. Engl. J. Med. *367*, 1694–1703.

Frantzias, J., Logan, J.G., Mollat, P., Sparatore, A., Del Soldato, P., Ralston, S.H., and Idris, A.I. (2012). Hydrogen sulphide-releasing diclofenac derivatives inhibit breast cancer-induced osteoclastogenesis in vitro and prevent osteolysis *ex vivo*. Br. J. Pharmacol. *165*, 1914–1925.

Guo, R., Wu, K., Chen, J., Mo, L., Hua, X., Zheng, D., Chen, P., Chen, G., Xu, W., and Feng, J. (2013). Exogenous hydrogen sulfide protects against doxorubicin-induced inflammation and cytotoxicity by inhibiting p38MAPK/NFkB pathway in H9c2 cardiac cells. Cell. Physiol. Biochem. *32*, 1668–1680.

Hauschild, A., Grob, J.J., Demidov, L.V. et al. (2012). Dabrafenib in BRAF-mutated metastatic melanoma: a multicentre, open-label, phase 3 randomised controlled trial. Lancet *380*, 358–365.

Hodi, F.S., O'Day, S.J., McDermott, D.F. et al. (2010). Improved survival with ipilimumab in patients with metastatic melanoma. N. Engl. J. Med. *363*, 711–723.

Hodis, E., Watson, I.R., Kryukov, G.V. et al. (2012). A landscape of driver mutations in melanoma. Cell *150*, 251–263.

Hu, L.F., Wong, P.T., Moore, P.K., and Bian, J.S. (2007). Hydrogen sulfide attenuates lipopolysaccharide-induced inflammation by inhibition of p38 mitogen-activated protein kinase in microglia. J. Neurochem. *100*, 1121–1128.

Ialenti, A., Di Meglio, P., D'Acquisto, F., Pisano, B., Maffia, P., Grassia, G., Di Rosa, M., and Ianaro, A. (2005). Inhibition of cyclooxygenase-2 gene expression by the heat shock response in J774 murine macrophages. Eur. J. Pharmacol. *509*, 89–96.

Ianaro, A., Tersigni, M., Belardo, G. et al. (2009). NEMO-binding domain peptide inhibits proliferation of human melanoma cells. Cancer Lett. *274*, 331–336.

Johannessen, C.M., Boehm, J.S., Kim, S.Y. et al. (2010). COT drives resistance to RAF inhibition through MAP kinase pathway reactivation. Nature *468*, 968–972.

© 2014 John Wiley & Sons A/S. Published by John Wiley & Sons Ltd

Jurkowska, H., Placha, W., Nagahara, N., and Wrobel, M. (2011). The expression and activity of cystathionine-gamma-lyase and 3-mercaptopyruvate sulfurtransferase in human neoplastic cell lines. Amino Acids *41*, 151–158.

Kantrow, S.M., Boyd, A.S., Ellis, D.L., Nanney, L.B., Richmond, A., Shyr, Y., and Robbins, J.B. (2007). Expression of activated Akt in benign nevi, Spitz nevi and melanomas. J. Cutan. Pathol. *34*, 593–596.

Lee, Z.W., Zhou, J., Chen, C.S., Zhao, Y., Tan, C.H., Li, L., Moore, P.K., and Deng, L.W. (2011). The slow-releasing hydrogen sulfide donor, GYY4137, exhibits novel anti-cancer effects in vitro and in vivo. PLoS ONE *6*, e21077.

Li, L., Rossoni, G., Sparatore, A., Lee, L.C., Del Soldato, P., and Moore, P.K. (2007). Anti-inflammatory and gastrointestinal effects of a novel diclofenac derivative. Free Radic. Biol. Med. *42*, 706–719.

Li, L., Fox, B., Keeble, J., Salto-Tellez, M., Winyard, P.G., Wood, M.E., Moore, P.K., and Whiteman, M. (2013). The complex effects of the slow-releasing hydrogen sulfide donor GYY4137 in a model of acute joint inflammation and in human cartilage cells. J. Cell Mol. Med. *17*, 365–376.

Nazarian, R., Shi, H., Wang, Q. et al. (2010). Melanomas acquire resistance to B-RAF(V600E) inhibition by RTK or N-RAS upregulation. Nature *468*, 973–977.

Oh, G.S., Pae, H.O., Lee, B.S., Kim, B.N., Kim, J.M., Kim, H.R., Jeon, S.B., Jeon, W.K., Chae, H.J., and Chung, H.T. (2006). Hydrogen sulfide inhibits nitric oxide production and nuclear factor-kB via heme oxygenase-1 expression in RAW264.7 macrophages stimulated with lipopolysaccharide. Free Radic. Biol. Med. *41*, 106–119.

Pan, L.L., Liu, X.H., Gong, Q.H., and Zhu, Y.Z. (2011). S-Propargyl-cysteine (SPRC) attenuated lipopolysaccharide-induced inflammatory response in H9c2 cells involved in a hydrogen sulfide-dependent mechanism. Amino Acids *41*, 205–215.

Pan, Y., Ye, S., Yuan, D., Zhang, J., Bai, Y., and Shao, C. (2012). Radioprotective role of H(2)S/CSE pathway in Chang liver cells. Mutat. Res. *738–739*, 12–18.

Panza, E., Tersigni, M., Iorizzi, M., Zollo, F., De Marino, S., Festa, C., Napolitano, M., Castello, G., Ialenti, A., and Ianaro, A. (2011). Lauroside B, a megastigmane glycoside from *Laurus nobilis* (bay laurel) leaves, induces apoptosis in human melanoma cell lines by inhibiting NF-kB activation. J. Nat. Prod. *74*, 228–233.

Poulikakos, P.I., Persaud, Y., Janakiraman, M. et al. (2011). RAF inhibitor resistance is mediated by dimerization of aberrantly spliced BRAF(V600E). Nature *480*, 387–390.

Scala, S., Giuliano, P., Ascierto, P.A. et al. (2006). Human melanoma metastases express functional CXCR4. Clin. Cancer Res. *12*, 2427–2433.

Sen, N., Paul, B.D., Gadalla, M.M., Mustafa, A.K., Sen, T., Xu, R., Kim, S., and Snyder, S.H. (2012). Hydrogen sulfide-linked sulfhydration of NF-kB mediates its antiapoptotic actions. Mol. Cell *45*, 13–24.

Shankar, S., Chen, Q., Ganapathy, S., Singh, K.P., and Srivastava, R.K. (2008). Diallyl trisulfide increases the effectiveness of TRAIL and inhibits prostate cancer growth in an orthotopic model: molecular mechanisms. Mol. Cancer Ther. *7*, 2328–2338.

Shi, H., Moriceau, G., Kong, X. et al. (2012). Melanoma whole-exome sequencing identifies (V600E)B-RAF amplification-mediated acquired B-RAF inhibitor resistance. Nat Commun *3*, 724.

Sivarajah, A., Collino, M., Yasin, M., Benetti, E., Gallicchio, M., Mazzon, E., Cuzzocrea, S., Fantozzi, R., and Thiemermann, C. (2009). Anti-apoptotic and anti-inflammatory effects of hydrogen sulfide in a rat model of regional myocardial I/R. Shock *31*, 267–274.

Sun, Q., Collins, R., Huang, S. et al. (2009). Structural basis for the inhibition mechanism of human cystathionine gamma-lyase, an enzyme responsible for the production of H(2)S. J. Biol. Chem. *284*, 3076–3085.

Szabo, C., Coletta, C., Chao, C., Modis, K., Szczesny, B., Papapetropoulos, A., and Hellmich, M.R. (2013). Tumor-derived hydrogen sulfide, produced by cystathionine-beta-synthase, stimulates bioenergetics, cell proliferation, and angiogenesis in colon cancer. Proc. Natl Acad. Sci. USA *110*, 12474–12479.

Taniguchi, S., Kang, L., Kimura, T., and Niki, I. (2011). Hydrogen sulphide protects mouse pancreatic beta-cells from cell death induced by oxidative stress, but not by endoplasmic reticulum stress. Br. J. Pharmacol. *162*, 1171–1178.

Tripatara, P., Patel, N.S., Collino, M. et al. (2008). Generation of endogenous hydrogen sulfide by cystathionine gamma-lyase limits renal ischemia/reperfusion injury and dysfunction. Lab. Invest. *88*, 1038–1048.

Ueda, Y., and Richmond, A. (2006). NF-kB activation in melanoma. Pigment Cell Res. *19*, 112–124.

Wallace, J.L., Caliendo, G., Santagada, V., Cirino, G., and Fiorucci, S. (2007). Gastrointestinal safety and anti-inflammatory effects of a hydrogen sulfide-releasing diclofenac derivative in the rat. Gastroenterology *132*, 261–271.

Wang, R. (2012). Physiological implications of hydrogen sulfide: a whiff exploration that blossomed. Physiol. Rev. *92*, 791–896.

Yang, G., Cao, K., Wu, L., and Wang, R. (2004). Cystathionine gamma-lyase overexpression inhibits cell proliferation via a H2S-dependent modulation of ERK1/2 phosphorylation and p21Cip/WAK-1. J. Biol. Chem. *279*, 49199–49205.

Supporting Information

Additional Supporting Information may be found in the online version of this article:

Table S1. Effect of H_2S-donors on PES 43, Sk-Mel-5 and Sk-Mel-28 melanoma cells proliferation.

Figure S1. Effect of hydrogen sulfide donors on A375 cell proliferation.

Figure S2. The hydrogen sulfide-releasing donor GYY4137 induced apoptosis and negatively regulated pro-survival pathways in melanoma cells.

© 2014 John Wiley & Sons A/S. Published by John Wiley & Sons Ltd